

ZGB model with random distribution of inert sites

G.L. HOENICKE AND W. FIGUEIREDO

Departamento de Física - Universidade Federal de Santa Catarina

88040-900, Florianópolis, SC - Brasil; e-mail: wagner@fisica.ufsc.br, hoenicke@fisica.ufsc.br

Abstract

A random distribution of inert sites is introduced in the Ziff-Gulari-Barshad model to study the phase transitions between active and poisoned states. The adsorption of CO and O₂ molecules is not possible at the position of the inert sites. This model is investigated in the site and pair approximations, as well as through Monte Carlo simulations. We determine the mean coverages of the elements as a function of the dilution and show that the continuous transition between the active and O-poisoned state is slightly affected by moderate values of dilution in the pair approximation and in the simulations. On the other hand, from the analysis of the hysteresis curves, the transition between the active and CO-poisoned states changes from first-order to continuous as one increases the concentration of inactive sites. The observed transition in the site and pair approximations is always of first-order nature. We also found the lines of transition and spinodal points as a function of the concentration of inert sites. Finally, the production rate of CO₂ is calculated as a function of the dilution of sites.

PACS number(s): 05.70.Ln, 05.70.Fh, 82.65.Jv, 82.20.Mj

I. INTRODUCTION

The study of nonequilibrium phase transitions is a topic of growing interest due to its application to a variety of complex systems^{1,2}: contact process, domain growth, catalysis, phase separation and transport phenomena. Although there is no general theory to account for nonequilibrium model systems, in recent years some progress has been achieved in understanding the stationary states of these systems employing approximate analytical methods and simulations. Some rigorous mathematical questions concerning the phase transitions of these complex interacting particle systems can be appreciated in the books of Liggett³ and Konno⁴.

In this paper we focus our attention on the phase transitions observed in the surface reaction model proposed by Ziff, Gulari and Barshad⁵ (ZGB), which describes some kinetic aspects of the oxidation of CO over a catalytic surface. In particular, here we consider a modified version of the ZGB model, where we incorporate a random distribution of inert sites on the catalytic surface. The original ZGB model is an irreversible lattice model for surface reactions based on the Langmuir-Hinshelwood mechanism, where the reactants must be adsorbed before reacting. The steps used to describe the ZGB model (a lattice Markov process) are the following: Molecules of CO and O₂ from a gaseous phase can be adsorbed onto the sites of a regular square lattice of identical sites. These molecules arrive at the surface according to their partial pressures in the gas mixture, that is, the probability of a CO molecule arriving is y_{co} and $(1 - y_{co})$ for the O₂ molecule. The CO molecule requires only a single vacant site to be adsorbed, while the O₂ is adsorbed if it finds a nearest-neighbor pair of empty sites. Upon adsorption, the O₂ molecule dissociates and the two free O atoms can react independently. If, after an adsorption step, a nearest-neighbor CO – O pair appears on the lattice, they immediately react, forming a CO₂ molecule that goes to the gas phase, leaving two empty sites on the lattice. Therefore, in this adsorption controlled limit, only a single parameter (y_{co}) is sufficient to describe the dynamics of the model.

The simulations performed by Ziff and co-workers have shown that the system exhibits

two phase transitions between active and poisoned states: for $y_{\text{co}} \leq y_1$, an O-poisoned state is formed, while for $y_{\text{co}} \geq y_2$ the lattice is poisoned by CO. For $y_1 < y_{\text{co}} < y_2$ a reactive steady-state is found, in which a nonzero number of vacant sites is present in the lattice. At y_1 the transition is continuous, whereas at y_2 the transition is of the first-order type. Using a mean field theory, Dickman⁶ qualitatively reproduced the phase diagram of the ZGB model and showed that, at the level of site approximation, only the first-order transition appears. However, employing the pair approximation, both continuous and first-order transitions are obtained.

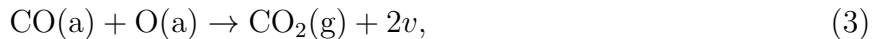
We are interested on the effects of inert sites on the phase transitions of the ZGB model. We have investigated in detail the dependence of the phase transitions on the concentration of inert sites. This problem presents some experimental interest in the automobile industry, where lead particles are deposited over the catalyst during the exhaust of the gases after combustion. This affects the efficiency of the catalytic surface due to the pinning of these lead particles on the surface, forbidding the adsorption of CO and O₂ molecules at the lead positions and reducing the reaction paths. Hovi and co-workers⁷, have studied by computer simulations the effect of preadsorbed poison and promoters on the irreversible ZGB model. They calculated the coverage of species as a function of the concentration of inert sites for a wide range of values, finding the interesting result that the first-order transition changes to a continuous one at a critical value of the concentration. Cortés and Valencia⁸ have also reported some results concerning random impurities distributed over the catalyst, in which they observed the change of the first-order transition into a continuous one as one increases the concentration of impurities. Albano⁹ simulated the ZGB model on incipient percolation clusters (IPC's) with a fractal dimension of 1.90. He showed that both transitions, at y_1 and y_2 are continuous, and that for an infinite lattice, in which y_{co} is larger than 0.408, the reactions stop at finite times because the IPC's are poisoned by pure CO. Casties et al.¹⁰ also performed a Monte Carlo simulation of the CO oxidation on probabilistic fractals. They observed a change in the character of the transition at y_2 from first order on regular lattices to second order on percolation clusters (for p larger than $p_c = 0.593$, which is the

percolation threshold on the square lattice).

In this work we have performed mean-field (site and pair approximations) calculations and Monte Carlo simulations for different values of the concentration of inert sites. The model studied here is a variant of the original ZGB model, where inert sites are randomly distributed over the lattice. Our approach is close related to that presented by Vigil and Willmore¹¹ to study the effects of spatial correlations on the oscillatory behavior of a modified ZGB model, where defects are continually added and desorbed from the surface. In their studies, they considered the mean-field site and pair approximations, as well as Monte Carlo simulations. In the present work we have determined the phase diagram for different concentrations, and the spinodal and transition lines as a function of the concentration of inert sites. We have constructed hysteresis curves to find the critical concentration at which the first-order transition changes into a continuous one. This paper is organized as follows: in Sec. II we present the results obtained within the site approximation; in Sec. III we introduce the pair approximation equations and show the results obtained using this scheme; Sec. IV presents the results of simulations, and finally, in Sec. V we present our conclusions.

II. SITE APPROXIMATION

We take a square lattice as our catalytic surface. A fraction n_d of the sites is randomly distributed over the lattice representing the pinned inert sites. The remaining sites of the lattice can be vacant, or occupied by either O atoms or CO molecules. The ZGB model is described by the following steps:



where the labels g and a denote the gaseous phase and an adsorbed reactant on the surface, respectively, and v indicates a vacant site. Steps (1) and (2) indicate the adsorption of the species, whereas the third step is the proper reaction, between distinct species located at adjacent sites of the lattice. In the site approximation the time evolution equations of the concentrations are given by

$$\frac{dn_o}{dt} = -y_{co}n_v(1 - (1 - n_o)^4) + 2(1 - y_{co})n_v^2(1 - n_{co})^3, \quad (4)$$

$$\frac{dn_{co}}{dt} = y_{co}n_v(1 - n_o)^4 - 2(1 - y_{co})n_v^2(1 - (1 - n_{co})^3), \quad (5)$$

where n_o , n_{co} and n_v represent, respectively, the coverages of O, CO and blank sites in the lattice. y_{co} gives the arrival probability of a CO molecule. In addition, there is the following constraint among the concentrations

$$n_{co} + n_o + n_v + n_d = 1. \quad (6)$$

The steady-state solutions of the above system of equations are given by $n_v = 0$, that corresponds to a poisoned surface, and

$$n_v = \frac{y_{co}}{2(1 - y_{co})} = Y. \quad (7)$$

Inserting Eq. (7) into Eq. (4) we obtain an expression for the steady-state values of the concentration n_{co} :

$$(n_{co} + Y + n_d)^4 + (1 - n_{co})^3 - 1 = 0. \quad (8)$$

We exhibit in Fig. 1 a typical diagram for the coverages of CO, O and vacant sites obtained for $n_d = 0.2$. This diagram was obtained by integrating the equations of motion for the n_{co} and n_o concentrations, starting from an initial condition in which the number of empty sites is $n_v = 1 - n_d$. The site approximation does not give any continuous transition for all values of the concentration of inert sites. This was already pointed out by Dickman⁶ for the ZGB model without inert sites. We observe in Fig. 1, that the limit of stability of the reactive phase is $y_s = 0.467510$, which corresponds to the spinodal point. Therefore, a

reactive steady-state is found for all values of $y_{\text{co}} \leq y_s$. For values of $y_{\text{co}} > y_s$, the system becomes poisoned, with a large amount of CO and a small concentration of O atoms. The presence of O atoms in the region $y_{\text{co}} > y_s$ is due to the inert sites that can block some oxygen, and also to the simplicity of the site approximation, which does not forbid the formation of O – CO nearest-neighbor pairs in the lattice. The tolerance of these O – CO pairs also explains the absence of the continuous phase transition, which is observed in the simulations. Fig. 2 is a plot of the solutions n_{co} of Eq.(8) versus the parameter Y for different values of concentration n_d of inert sites. We obtain two solutions, which we call $n_{\text{co}}^>$ and $n_{\text{co}}^<$, that join together at the spinodal point. For instance, for $n_d = 0$ the value we find is $Y = 0.638986$, which furnishes the value $y_s = 0.561013$. We also note in Fig. 2 that, at the spinodal point, the concentration of n_{co} molecules remains the same irrespective of the value we choose for n_d . This special value is $n_{\text{co}} = 0.1660$. Then, the net effect of adding n_d is to shift the curves horizontally. In this site approximation, solutions are possible only for values of $n_d < 0.638986$. This happens because above this value the solution would correspond to the non-physical value $y_{\text{co}} < 0$. So, the meaning of the two solutions in Fig. 2 is the following: the branch $n_{\text{co}}^<$ represents the stable steady-state solutions whereas the $n_{\text{co}}^>$ branch gives the unstable solutions. These solutions were obtained after numerical integration of the equations of motion for n_{co} and n_o , starting from the state described by $n_v = 1 - n_d$. For the initial condition $n_v = Y$ and n_{co} larger than $n_{\text{co}}^>$ the system evolves to the poisoned state. The initial condition $n_v = Y$ and n_{co} less than $n_{\text{co}}^>$ drives the system to the lower stable reactive solution $n_{\text{co}}^<$.

Fig. 2 also shows that, as we approach the spinodal point for any value of n_d , the region of stability becomes narrower. Then, we expect that for some value of $y_{\text{co}} \leq y_s$ a first-order transition occurs, that is, the concentration n_{co} must increase abruptly from a small value (reactive phase) to a large value (poisoned phase). Unfortunately, we cannot use here the usual thermodynamic considerations based on the minimization of a suitable thermodynamic potential. In order to find this first-order transition we adopt the same kinetic criteria employed by Dickman⁶, which was borrowed from the work of Ziff et al⁵.

The phase transition was determined by choosing an initial state where half of the lattice was empty and the other half was completely filled with CO. In this work we choose as our initial state, to solve the equations of motion for n_{co} and n_o , the values $n_v = n_{co} = \frac{1}{2}(1 - n_d)$. It is clear that this choice is not the same as that considered by Ziff et al., because we cannot discriminate which sites are empty or not. The phase boundary is defined at the special value y_2 where the solution of the equations of motion changes from the reactive to the poisoned state as we vary the value of y_{co} for the same initial condition, as established above. For $n_d = 0$ we obtain the same value found by Dickman. We exhibit in Fig. 3 the results obtained for the first-order transition and the spinodal points for $n_d = 0.2$. The spinodal was obtained from the initial condition $n_v = 1 - n_d$, and the first-order transition from the condition $n_v = n_{co} = \frac{1}{2}(1 - n_d)$. For this particular value of $n_d = 0.2$, we have $y_2 = 0.3999$ and $y_s = 0.4821$. We have considered all values of the concentration of inert sites, and Fig. 4 shows the values of y_s (dashed line) and y_2 (full line) as a function of the concentration of inert sites. At the particular value $n_d = 0.55$ the two lines merge. For values of $n_d > 0.55$ the transition still remains of the first-order type, although the number of vacant sites that stay in the active state is very small. For instance, for $n_d = 0.60$, at the transition point ($y_2 = 0.0725$), the number of vacant sites changes from 0.0388 in the active state, to 2×10^{-8} in the poisoned state. Throughout our analysis we considered a given state to be active if the number of vacant sites is larger than 10^{-6} . We also exhibit in Fig. 5 the number of vacant sites n_v at the active state as a function of the number of inert sites n_d , at the transition and spinodal points. We observe that for all values of $n_d < 0.55$, the number of vacant sites at the spinodal point is always larger than that at the transition point.

III. PAIR APPROXIMATION

Let us consider the application of the pair approximation procedure to this ZGB model that includes inert sites. Here we introduce the pair probability $P_{\alpha\beta}$ of a random nearest

neighbor pair of sites being occupied by species α and β . We have the following types of species: v , d , c , and O , which represent, respectively, vacant, inert, carbon monoxide, and oxygen. As in the previous treatments^{12,13} we need to consider only the changes that occur at a particular central pair in the lattice. In the table below we display the allowed and forbidden (indicated by \times) nearest-neighbor pairs in the present model.

	v	o	c	d
v	vv	vo	vc	vd
o		oo	\times	od
c		\times	cc	cd
d				dd

The next table also exhibits all the possible transitions among pairs. We obtain 14 independent transitions, labelled by numbers in the range 1 – 14. In the table transitions indicated by \times are prohibited.

$\frac{\text{from} \rightarrow}{\text{to} \downarrow}$	vv	vo	vc	vd	oo	od	cc	cd
vv		4	6	\times	\times	\times	12	\times
vo	1		\times	\times	10	\times	\times	\times
vc	2	\times		\times	\times	\times	13	\times
vd	\times	\times	\times		\times	11	\times	14
oo	3	5	\times	\times		\times	\times	\times
od	\times	\times	\times	8	\times		\times	\times
cc	\times	\times	7	\times	\times	\times		\times
cd	\times	\times	\times	9	\times	\times	\times	

Then, we write the equations relating the probability of each element with the corresponding pair probabilities:

$$\begin{aligned}
P_v &= P_{vv} + P_{vo} + P_{vc} + P_{vd}, \\
P_o &= P_{od} + P_{vo} + P_{oo} \quad , \\
P_c &= P_{cd} + P_{vc} + P_{cc} \quad , \\
P_d &= P_{dd} + P_{vd} + P_{od} + P_{cd}.
\end{aligned} \tag{9}$$

The pair probabilities also satisfy the constraint

$$P_{vv} + P_{oo} + P_{cc} + P_{dd} + 2(P_{vo} + P_{vc} + P_{vd} + P_{od} + P_{cd}) = 1. \tag{10}$$

Next, we need to write the time evolution equations for the pair probabilities. Examining the latter table we can construct the desired equations of evolution. We explicitly write the equations of motion for the pair probabilities $P_{\alpha\beta}$.

$$\begin{aligned}
\frac{dP_{vo}}{dt} &= t_1 + t_{10} - t_4 - t_5, \\
\frac{dP_{vc}}{dt} &= t_2 + t_{13} - t_6 - t_7, \\
\frac{dP_{vd}}{dt} &= t_{11} + t_{14} - t_8 - t_9, \\
\frac{dP_{oo}}{dt} &= t_3 + 2t_5 - 2t_{10}, \\
\frac{dP_{od}}{dt} &= t_8 - t_{11}, \\
\frac{dP_{cc}}{dt} &= 2t_7 - t_{12} - 2t_{13}, \\
\frac{dP_{cd}}{dt} &= t_9 - t_{14}, \\
\frac{dP_{vv}}{dt} &= -t_3 + t_{12} - 2t_1 + 2t_4 - 2t_2 + 2t_6, \\
\frac{dP_{dd}}{dt} &= 0.
\end{aligned} \tag{11}$$

where t_1 to t_{14} are the transition rates. The factors of two arising in the equation of motion for P_{vv} are due to the fact that the pair probabilities P_{ij} and P_{ji} are equal by symmetry. For instance, from the pair vv we can obtain, with the same probability, the different configurations ov and vo . In general, the expressions for the transition rates are lengthy, and we present these transition rates in the Appendix.

In this pair approximation we cannot obtain analytical solutions as we have done in the site approximation. We solved the coupled set of eight nonlinear equations by the fourth-

order Runge-Kutta method, searching for the stationary solutions. We considered the two different initial conditions as in the case of the site approximation.

Let us first consider the evolution from the initial state where $P_v = 1 - P_d$, in which only the pairs vv , vd and dd are present in the lattice at $t = 0$. Figure 6 shows the diagram of the model for $P_d = 0.2$. For $0 < y_{co} \leq 0.2299$ the lattice poisons with oxygen. In the range $0.2299 < y_{co} < 0.4821$ there is an active region, and for $y_{co} \geq 0.4821$ the lattice poisons with CO. When $P_d = 0$, we found the same figures obtained by Dickman in his pair approximation. For instance, the site and pair approximations give the same value for the spinodal point y_s . However, when we consider some inert sites in the lattice, the spinodal point found in the site approximation is always smaller than that obtained within the pair approximation. For this particular value, $P_d = 0.2$, the site approximation yields $y_s = 0.4675$, whereas $y_s = 0.4821$ is obtained by the pair approximation. The value of y_{co} at the continuous transition, which now arises in this pair approximation, decreases slightly with increasing values of the concentration of inert sites.

We also considered the solutions evolving from an initial condition where half of the free sites ($P_v = 1 - P_d$) is filled with CO molecules and the other half left empty. In order to be close to the initial condition used in the simulation, we chose for the initial pair conditions $P_{cc} = P_{vv}$, $P_{dv} = P_{dc}$ and $P_{vc} = 0$, which mimics a division of the lattice into two parts: on one side of the lattice we would have inert sites and CO molecules and, on the other side, vacant and inert sites. If $P_d = 0$, we found for the transition between the active and CO-poisoned states the value $y_2 = 0.5240$, which agrees with the value found in the simulations. Fig. 7 displays the concentration of CO molecules at the transition point for which $P_d = 0.2$. In this pair approximation, the values of y_s and y_2 are very close. We also show in Fig. 8 the concentration of vacant sites as a function of the concentration of inert sites, at the transition point, and also at the spinodal point. Both curves join at $P_d = 0.50$, and for $P_d > 0.60$, we cannot observe any active state. As in the site approximation, an active state is defined only if $P_v > 10^{-6}$. Then, the calculations performed within the pair approximation give results that are very similar to those obtained by the site approximation,

concerning the spinodal and transition points.

In addition, it was observed that initial conditions do not affect the point in which the continuous phase transition occurs. In Fig. 9 we exhibit the phase diagram for this ZGB model with inert sites. The size of the reactive window decreases as we increase the concentration of inert sites. We have plotted the transition line for the first-order transition and for the spinodal line, which gives the limit of stability of the reactive phase. The line separating the active and O-poisoned phases is a continuous transition line.

IV. SIMULATIONS

We have performed Monte Carlo simulations in the ZGB model with inert sites in order to check the results we have obtained in the site and pair approximations. The simulations were carried for different values of the concentration of inert sites P_d . For small values of P_d , we considered square lattices of linear size $L = 64$, but for large values of P_d we have used lattices of linear size up to $L = 150$. The first step in the simulation is to randomly distribute the selected fraction P_d of inert sites in the lattice. All simulations then started with a fraction of empty sites equal to $P_v = 1 - P_d$. The CO molecules arrive at the surface with a probability y_{co} and the O₂ molecules with probability $1 - y_{co}$. The rules for adsorption and reaction of the species are exactly the same as in the original ZGB model⁵. Since adsorption of oxygen requires two nearest neighbor empty sites, the effect of the inert sites is to favour the adsorption of CO relatively to that of O₂ molecules. In general, we have taken 10^3 Monte Carlo steps (MCs) to attain the stationary states, and 10^3 more to calculate the concentration averages at the stationary states. One MCs is equal to $L \times L$ trials of deposition of species, where L is the linear size of the lattice. To speed up the simulations we worked with a suitable list of empty sites.

We exhibit in Fig. 10 the phase diagram of the model in the plane y_{co} versus P_d . It is similar to that obtained within the pair approximation. However, there is a fundamental difference between the transition line separating the active and CO-poisoned phases in both

approaches. In the pair approximation the transition line is always of the first-order type, whereas in the simulations there is a critical concentration above which the transition becomes continuous. We have done detailed simulations to find the critical concentration at which the transition becomes continuous. We have found for the critical concentration of inert sites the value $P_d^c = 0.078$. We arrived at this value by looking at the hysteresis loops in the curves of P_{co} versus y_{co} for different values of the concentration P_d , as we can see in Fig. 11. We proceed as follows: in Fig. 11a we fixed the concentration of inert sites at the value 0.070 and the curve with circles, which is the proper transition curve, was obtained from an initial state where $P_v = 1 - P_d$, that is, with a lattice almost empty. The curve with squares was determined from an initial state in which the lattice was almost covered by CO. We have taken a fraction of only 5% of randomly empty sites over the lattice at the starting time. Then, we clearly observe the hysteresis loop at the concentration P_d , which implies that the transition is of first-order. On the other hand, Fig. 11b, where the fraction of inert sites is $P_d = 0.080$, does not exhibit the hysteresis loop and the transition is clearly a continuous one. The critical value of $P_d^c = 0.078$ was obtained analysing the behavior of these curves in the range $0.070 < P_d < 0.080$. As we have pointed out in the Introduction, Hovi et al.⁷ had already observed the change in the nature of this transition as a function of the concentration. The phase boundary separating the active and the O-poisoned phases in Fig. 10 is continuous for all values of P_d . We have checked this fact by observing that no hysteresis loop was found for any value of P_d . The width of the active phase decreases with increasing values of P_d . For values of $P_d > 0.45$ the lattice is poisoned (absence of empty sites) with different amounts of CO and O species. Due to finite size effects, this value is larger than the value 0.408 found by Albano⁹ in the limit of very large IPC's.

We have also noted that the production rate of CO₂ molecules attains its maximum value exactly at the first-order transition, for values of $P_d < P_d^c$. If $P_d > P_d^c$ the maximum production rate of CO₂ molecules is located inside of the reactive window. This is seen in Fig. 12, where the circles indicate the points where the production rate of CO₂ is maximum. In the site and pair approximations this maximum occurs always at the phase boundary,

irrespective of the value of P_d . Fig. 13 shows the production rate R of CO_2 molecules as a function of P_d . As expected, the role of inert sites is also of blocking the reactions over the catalyst. The maximum production rate occurs at a surface free of impurities.

V. CONCLUSIONS

We have studied the effects of a random distribution of inert sites on the phase diagram of the ZGB model. We determined the time evolution equations for the concentrations of the different species over the catalytic surface within an effective field theory, at the level of site and pair approximations, and also performed Monte Carlo simulations on the model. We obtained the coverages of the species as function of the deposition rate of CO and of the concentration of inert sites. In the site and pair approximations we found the transition line and the limit of stability of the reactive phase. In the site approximation, the continuous transition between the O-poisoned and reactive states is absent for any values of the concentration of inert sites. The width of the reactive window exhibits the same behavior, as a function of concentration of inert sites, in both pair approximation and Monte Carlo simulations. However, the transition between the reactive and CO-poisoned phase is always of first-order in the site and pair approximations, whereas Monte Carlo simulations give a critical point where the transition changes nature. For values of the concentration of inert sites less than the critical value, the transition is first-order and above this value, it changes to a continuous one. The determination of this critical concentration was possible through the analysis of the hysteresis curves for different values of the concentration of inert sites. The production rate of CO_2 molecules is maximum at the first-order transition, in both site and pair approximations. This is the case in the simulations, but the transition is of the first-order type. When the concentration of inert sites is greater than the critical value, the maximum production rate of CO_2 molecules moves towards the reactive window. The overall effect of inert sites is to reduce the production of CO_2 molecules.

ACKNOWLEDGMENTS

We would like to thank Ron Dickman by his many valuable suggestions, and Luis G. C. Rego by the critical reading of the manuscript. This work was supported by the Brazilian agencies CAPES, CNPq and FINEP.

APPENDIX: TRANSITION RATES IN THE PAIR APPROXIMATION

We present the transition rates in the pair approximation, which we used in Section III to solve the time evolution equations for the pair probabilities. The transition rates are t_1 to t_{14} , which are given by

$$t_1 = t_{1a} + t_{1b} \tag{A1}$$

$$t_{1a} = (1 - y_{co})P_{vv}3\frac{P_{vv}}{P_v}\left(1 - \frac{P_{vc}}{P_v}\right)^2$$

$$t_{1b} = (1 - y_{co})P_{vv}\left(1 - \frac{P_{vc}}{P_v}\right)^3\left\{1 - \left(1 - \frac{P_{vc}}{P_v}\right)^3\right\}$$

$$t_2 = y_{co}P_{vv}\left(1 - \frac{P_{vo}}{P_v}\right)^3 \tag{A2}$$

$$t_3 = (1 - y_{co})P_{vv}\left(1 - \frac{P_{vc}}{P_v}\right)^6 \tag{A3}$$

$$t_4 = t_{4a} + t_{4b} \tag{A4}$$

$$t_{4a} = y_{co}P_{vo}\left\{\left(1 - \frac{P_{vo}}{P_v}\right)^3 + \frac{3}{2}\frac{P_{vo}}{P_v}\left(1 - \frac{P_{vo}}{P_v}\right)^2 + \left(\frac{P_{vo}}{P_v}\right)^2\left(1 - \frac{P_{vo}}{P_v}\right)\frac{1}{4}\left(\frac{P_{vo}}{P_v}\right)^3\right\}$$

$$t_{4b} = y_{co}P_{vo}\left\{3\frac{P_{vo}}{P_o}\left[\left(1 - \frac{P_{vo}}{P_v}\right)^3 + \frac{3}{2}\frac{P_{vo}}{P_v}\left(1 - \frac{P_{vo}}{P_v}\right)^2 + \left(\frac{P_{vo}}{P_v}\right)^2\left(1 - \frac{P_{vo}}{P_v}\right) + \frac{1}{4}\left(\frac{P_{vo}}{P_v}\right)^3\right]\right\}$$

$$t_5 = (1 - y_{co})P_{vo}3\frac{P_{vv}}{P_v}\left(1 - \frac{P_{vc}}{P_v}\right)^2 \tag{A5}$$

$$t_6 = t_{6a} + t_{6b} \quad (\text{A6})$$

$$t_{6a} = (1 - y_{co})P_{vc}3\frac{P_{vv}}{P_v}\left\{\left(1 - \frac{P_{vc}}{P_v}\right)^2 + \frac{P_{vc}}{P_v}\left(1 - \frac{P_{vc}}{P_v}\right) + \frac{1}{3}\left(\frac{P_{vc}}{P_v}\right)^2\right\}$$

$$t_{6b} = 3(1 - y_{co})P_{vc}\frac{P_{vc}}{P_c}\left\{3\frac{P_{vv}}{P_v}\left[\left(1 - \frac{P_{vc}}{P_v}\right)^2 + \frac{P_{vc}}{P_v}\left(1 - \frac{P_{vc}}{P_v}\right) + \frac{1}{3}\left(\frac{P_{vc}}{P_v}\right)^2\right]\right\}$$

$$t_7 = y_{co}P_{vc}\left(1 - \frac{P_{vo}}{P_v}\right)^3 \quad (\text{A7})$$

$$t_8 = (1 - y_{co})P_{vd}3\frac{P_{vv}}{P_v}\left(1 - \frac{P_{vc}}{P_v}\right)^2 \quad (\text{A8})$$

$$t_9 = y_{co}P_{vd}\left(1 - \frac{P_{vo}}{P_v}\right)^3 \quad (\text{A9})$$

$$t_{10} = t_{10a} + t_{10b} \quad (\text{A10})$$

$$t_{10a} = y_{co}P_{oo}\frac{P_{vo}}{P_o}\left\{\left(1 - \frac{P_{vo}}{P_v}\right)^3 + \frac{2}{3}\frac{P_{vo}}{P_v}\left(1 - \frac{P_{vo}}{P_v}\right)^2 + \left(\frac{P_{vo}}{P_v}\right)^2\left(1 - \frac{P_{vo}}{P_v}\right) + \frac{1}{4}\left(\frac{P_{vo}}{P_v}\right)^3\right\}$$

$$t_{10b} = 2y_{co}P_{oo}\frac{P_{vo}}{P_o}\left\{\left(1 - \frac{P_{vo}}{P_v}\right)^2\left(1 - \frac{P_{oo}}{P_o}\right) + \frac{1}{2}\left[\frac{P_{oo}}{P_o}\left(1 - \frac{P_{vo}}{P_v}\right)^2 + 2\frac{P_{vo}}{P_v}\left(1 - \frac{P_{vo}}{P_v}\right)\left(1 - \frac{P_{oo}}{P_o}\right)\right] + \frac{1}{3}\left(\frac{P_{vo}}{P_v}\right)^2\left(1 - \frac{P_{oo}}{P_o}\right) + \frac{2}{3}\frac{P_{vo}}{P_v}\left(1 - \frac{P_{vo}}{P_v}\right)\frac{P_{oo}}{P_o} + \frac{1}{4}\left(\frac{P_{vo}}{P_v}\right)^2\frac{P_{oo}}{P_o}\right\}$$

$$t_{11} = t_{11a} + t_{11b} \quad (\text{A11})$$

$$t_{11a} = y_{co}P_{od}\frac{P_{vo}}{P_o}\left\{\left(1 - \frac{P_{vo}}{P_v}\right)^3 + \frac{3}{2}\frac{P_{vo}}{P_v}\left(1 - \frac{P_{vo}}{P_v}\right)^2 + \left(\frac{P_{vo}}{P_v}\right)^2\left(1 - \frac{P_{vo}}{P_v}\right) + \frac{1}{4}\left(\frac{P_{vo}}{P_v}\right)^3\right\}$$

$$t_{11b} = 2y_{co}P_{od}\frac{P_{vo}}{P_o}\left\{\left(1 - \frac{P_{vo}}{P_v}\right)^2\left(1 - \frac{P_{od}}{P_d}\right) + \frac{1}{2}\left(1 - \frac{P_{vo}}{P_v}\right)^2\frac{P_{od}}{P_d} + \frac{P_{vo}}{P_v}\left(1 - \frac{P_{vo}}{P_v}\right)\left(1 - \frac{P_{od}}{P_d}\right) + \frac{1}{3}\left(\frac{P_{vo}}{P_v}\right)^2\left(1 - \frac{P_{od}}{P_d}\right) + \frac{2}{3}\frac{P_{vo}}{P_v}\left(1 - \frac{P_{vo}}{P_v}\right)\frac{P_{od}}{P_d} + \frac{1}{4}\left(\frac{P_{vo}}{P_v}\right)^2\frac{P_{od}}{P_d}\right\}$$

$$\begin{aligned}
t_{12} = & 2(1 - y_{co})P_{cc} \left(\frac{P_{vc}}{P_c} \right)^2 \left\{ \left(1 - \frac{P_{vc}}{P_v} \right)^4 + 2 \left(1 - \frac{P_{vc}}{P_v} \right)^3 \frac{P_{vc}}{P_v} \right. \\
& + \frac{2}{3} \left(\frac{P_{vc}}{P_v} \right)^2 \left(1 - \frac{P_{vc}}{P_v} \right)^2 + \left(\frac{P_{vc}}{P_v} \right)^2 \left(1 - \frac{P_{vc}}{P_v} \right)^2 \\
& \left. + \frac{2}{3} \left(\frac{P_{vc}}{P_v} \right)^3 \left(1 - \frac{P_{vc}}{P_v} \right) + \frac{1}{9} \left(\frac{P_{vc}}{P_v} \right)^4 \right\}
\end{aligned} \tag{A12}$$

$$\begin{aligned}
t_{13} &= t_{13a} + t_{13b} \\
t_{13a} &= (1 - y_{co})P_{cc} \frac{P_{vc}}{P_c} 3 \frac{P_{vv}}{P_v} \left\{ \left(1 - \frac{P_{vc}}{P_v} \right)^2 + \frac{P_{vc}}{P_v} \left(1 - \frac{P_{vc}}{P_v} \right) + \frac{1}{3} \left(\frac{P_{vc}}{P_v} \right)^2 \right\} \\
t_{13b} &= 2(1 - y_{co})P_{cc} \frac{P_{vc}}{P_c} \left\{ 2 \frac{P_{vv}}{P_v} \left[\left(1 - \frac{P_{vc}}{P_v} \right) \left(1 - \frac{P_{cc}}{P_c} \right) + \frac{1}{2} \frac{P_{vc}}{P_v} \left(1 - \frac{P_{cc}}{P_c} \right) \right. \right. \\
& + \frac{1}{2} \left(1 - \frac{P_{vc}}{P_v} \right) \frac{P_{cc}}{P_c} + \frac{1}{3} \frac{P_{vc}}{P_v} \frac{P_{cc}}{P_c} \left. \right] + \frac{P_{vc}}{P_c} \left[\left(1 - \frac{P_{vc}}{P_v} \right)^2 \right. \\
& \left. \left. + \frac{P_{vc}}{P_v} \left(1 - \frac{P_{vc}}{P_v} \right) + \frac{1}{3} \left(\frac{P_{vc}}{P_v} \right)^2 \right] \right\} \times \left[\frac{P_{vc}}{P_v} \left(1 - \frac{P_{vc}}{P_v} \right) + \frac{2}{3} \left(\frac{P_{vc}}{P_v} \right)^2 \right]
\end{aligned} \tag{A13}$$

$$\begin{aligned}
t_{14} &= t_{14a} + t_{14b} \\
t_{14a} &= (1 - y_{co})P_{cd} \frac{P_{vc}}{P_c} \left\{ 3 \frac{P_{vv}}{P_v} \left[\left(1 - \frac{P_{vc}}{P_v} \right)^2 + \frac{P_{vc}}{P_v} \left(1 - \frac{P_{vc}}{P_v} \right) + \frac{1}{3} \left(\frac{P_{vc}}{P_v} \right)^2 \right] \right\} \\
t_{14b} &= 2(1 - y_{co})P_{cd} \frac{P_{vc}}{P_c} \left\{ 2 \frac{P_{vv}}{P_v} \left[\left(1 - \frac{P_{vc}}{P_v} \right) \left(1 - \frac{P_{cd}}{P_d} \right) + \frac{1}{2} \frac{P_{vc}}{P_v} \left(1 - \frac{P_{cd}}{P_d} \right) \right. \right. \\
& + \frac{1}{2} \left(1 - \frac{P_{vc}}{P_v} \right) \frac{P_{cd}}{P_d} + \frac{1}{3} \frac{P_{vc}}{P_v} \frac{P_{cd}}{P_d} \left. \right] + \frac{P_{vd}}{P_d} \left(1 - \frac{P_{vc}}{P_v} \right)^2 + \frac{2}{2} \frac{P_{vc}}{P_v} \frac{P_{vd}}{P_d} \\
& \left. \left. + \frac{1}{3} \left(\frac{P_{vc}}{P_v} \right)^2 \right] \right\}
\end{aligned} \tag{A14}$$

REFERENCES

- [1] J. Marro and R. Dickman, *Nonequilibrium Phase Transitions in Lattice Models* (Cambridge University Press, Cambridge, 1999).
- [2] V. Privman, ed., *Nonequilibrium Statistical Mechanics in One Dimension* (Cambridge University Press, Cambridge, 1996).
- [3] T.M. Liggett, *Interacting Particle Systems* (Springer-Verlag, New York, 1985).
- [4] N. Konno, *Phase Transitions of Interacting Particle Systems* (World Scientific, Singapore, 1994).
- [5] R. M. Ziff, E. Gulari, and Y. Barshad, Phys. Rev. Lett. **56**, 2553 (1986).
- [6] R. Dickman, Phys. Rev. A **34**, 4246 (1986).
- [7] J. -P. Hovi, J. Vaari, H. -P. Kaukonen and R.M. Nieminen, Compt. Mater. Science, **1**, 33 (1992).
- [8] Joaquin Cortés and Eliana Valencia, Surf. Sci. **425**, L357 (1999).
- [9] E.V. Albano, Phys. Rev. B **42**, 10818 (1990).
- [10] A. Casties, J. Mai, and W. von Niessen, J. Chem. Phys. **99**, 3082 (1993).
- [11] R. Dennis Vigil and Frank T. Willmore, Phys. Rev. E **54**, 1225 (1996).
- [12] A.G. Dickman, B.C.S. Grandi, W. Figueiredo and R. Dickman, Phys. Rev. E **59**, 6361 (1999).
- [13] E.C. da Costa and W. Figueiredo, Phys. Rev. E **61**, 1134 (2000).

FIGURES

FIG. 1. Coverages of CO (full line), O (dashed line) and empty sites (dotted line), as a function of the deposition rate of CO. The concentration of inert sites is $n_d = 0.2$. Coverages obtained through the site approximation.

FIG. 2. Stability curves in the site approximation for different values of concentration of inert sites. The upper ($n_{co}^>$) and lower ($n_{co}^<$) branches give the concentration of CO, respectively, at the unstable and stable states. The open circles indicate the position of the spinodal points. From the outer to the inner curves the concentration of inert sites is 0.0, 0.1, 0.2, 0.3, 0.4, 0.5 and 0.6.

$$Y = \frac{y_{co}}{2(1-y_{co})}.$$

FIG. 3. Plots of the concentration of CO (n_{co}) versus y_{co} to locate the spinodal and transition points for the particular value $n_d = 0.2$. Spinodal (dashed line), first-order transition (full line).

FIG. 4. Behavior of the spinodal (dashed) and first-order transition (full) lines as a function of concentration of inert sites in the site approximation.

FIG. 5. Concentration of empty sites at the spinodal (dashed line) and at the first-order transition (full line) as a function of the concentration of inert sites.

FIG. 6. The same legend as in Figure 1, but coverages obtained within pair approximation.

FIG. 7. The same legend as in Fig. 3. Calculations performed in the pair approximation. P_{co} has the same meaning that n_{co} .

FIG. 8. Concentration of vacant sites at the spinodal (dashed line) and at the first-order transition (full line) as a function of the concentration of inert sites, in the pair approximation.

FIG. 9. Phase diagram of the ZGB model with inert sites. P_d gives the concentration of inert sites, y_{co} is the probability that the CO molecule hits the surface. We have an active phase and a O-poisoned and CO-poisoned phases. The dashed line represents the spinodal points, the full line, the first-order transition points, and the dotted line gives the continuous transition points. Phase diagram obtained in the pair approximation.

FIG. 10. Phase diagram in the plane P_d versus y_{co} , obtained through Monte Carlo simulations showing the reactive window. The squares give the transition between the reactive and CO-poisoned phases. The circles represent the continuous transitions between the active and O-poisoned phases. The lines are a guide to the eyes.

FIG. 11. Hysteresis curves near the critical value of the concentration of inert sites. (a) $P_d = 0.070$, (b) $P_d = 0.080$.

FIG. 12. Plot of P_d versus y_{co} showing the points where the production rate of CO_2 is maximum (circles), and the production (squares) at the transition between the active and CO-poisoned phases. The lines serve as a guide to the eyes.

FIG. 13. Maximum production rate of CO_2 molecules (R) as a function of the concentration of inert sites P_d .

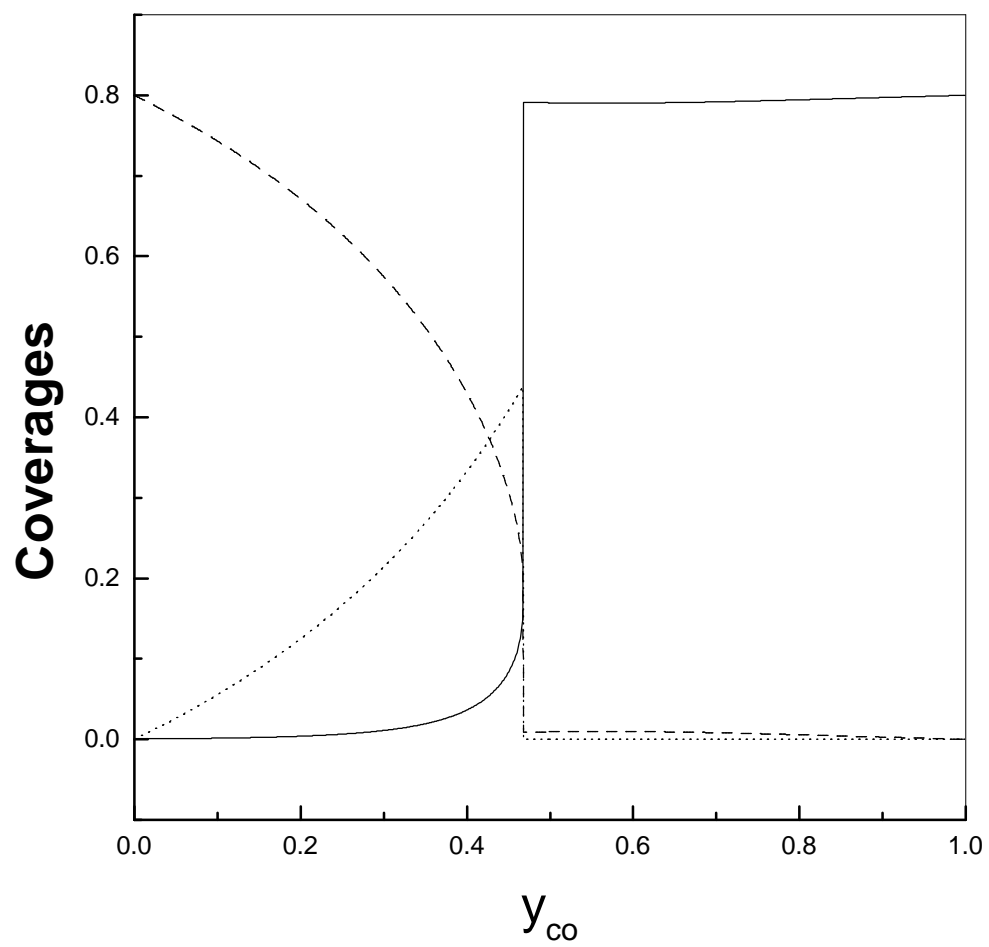


Fig. 1 - Hoenicke + Figueiredo

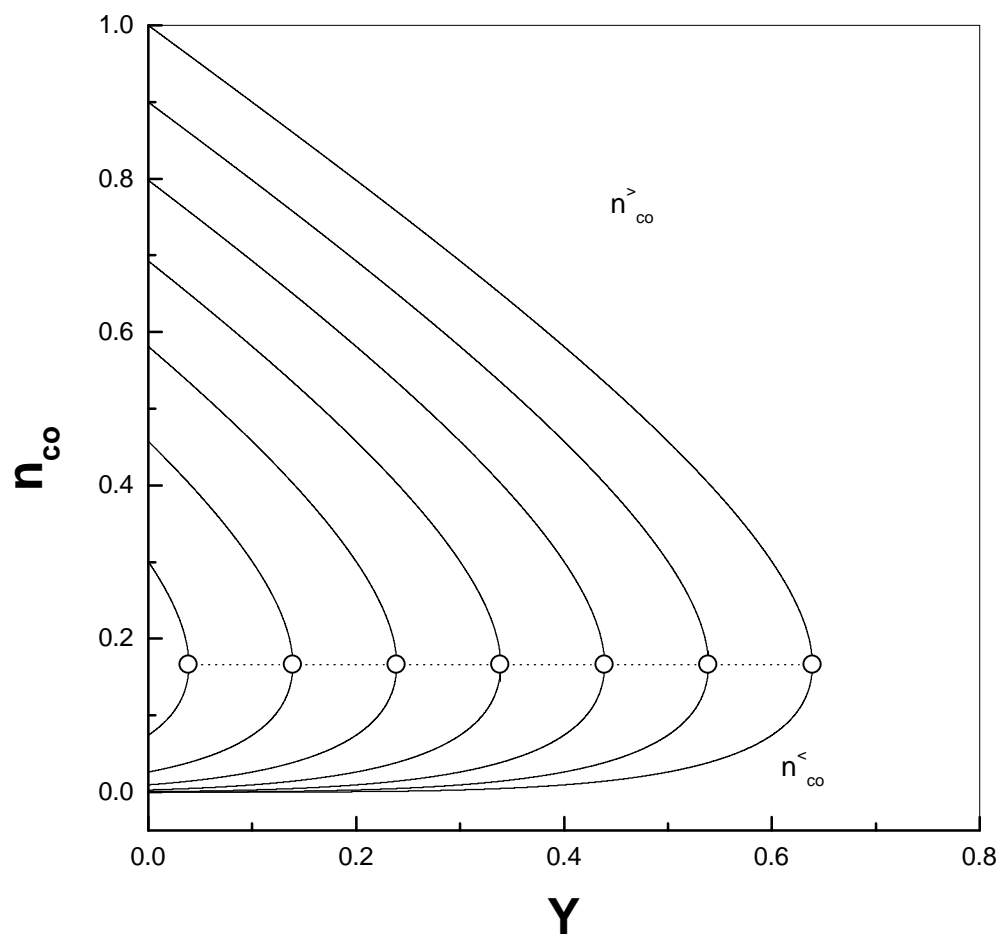


Fig. 2 - Hoenicke + Figueiredo

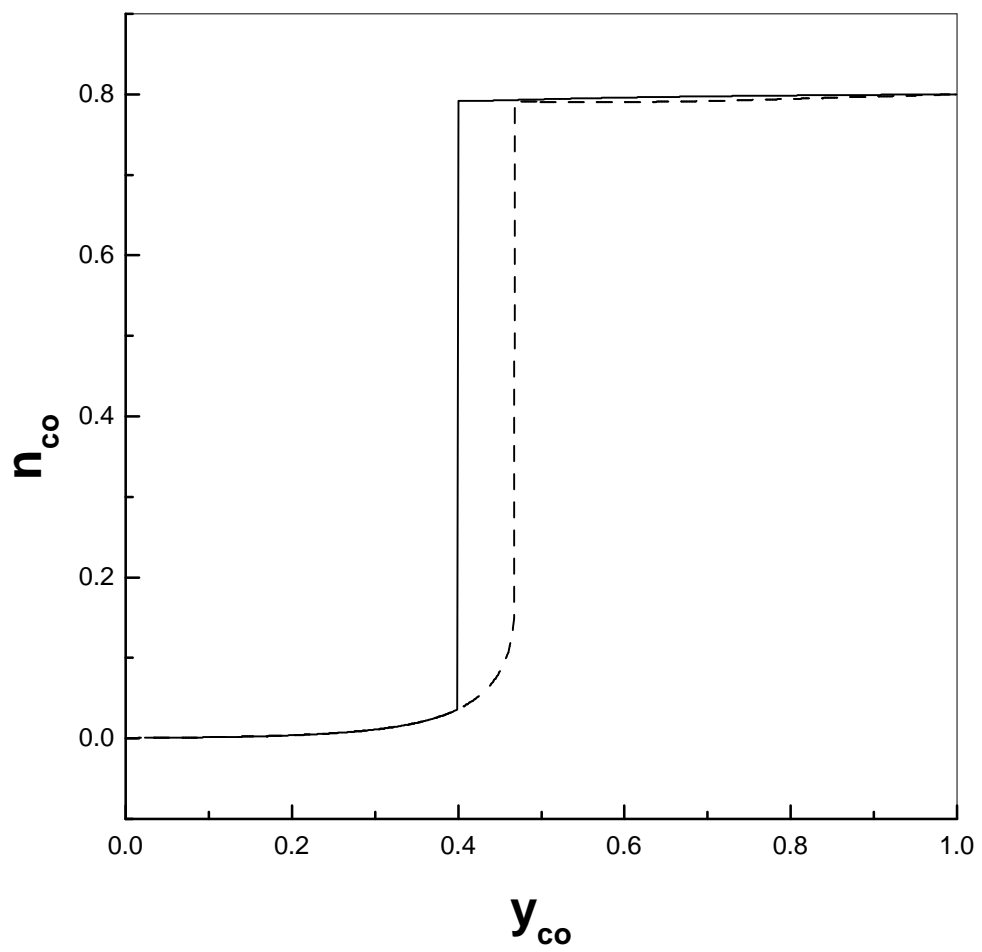


Fig. 3 - Hoenicke + Figueiredo

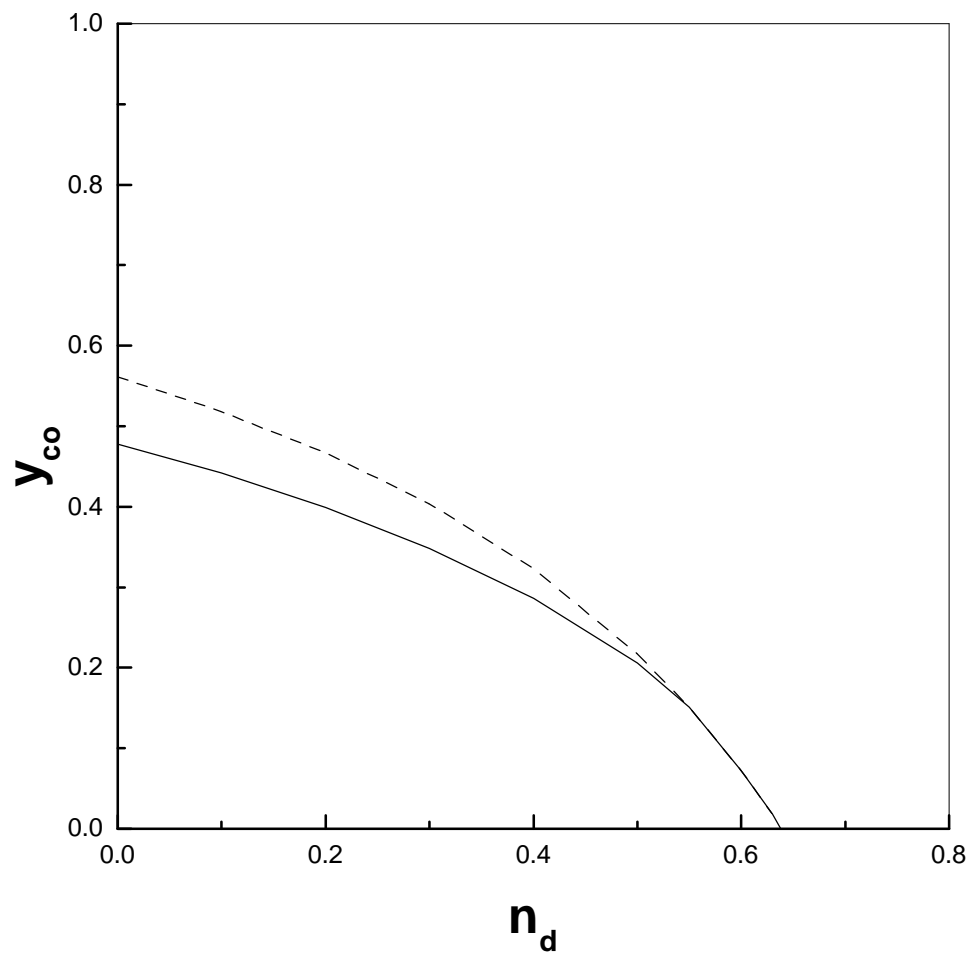


Fig. 4 - Hoenicke + Figueiredo

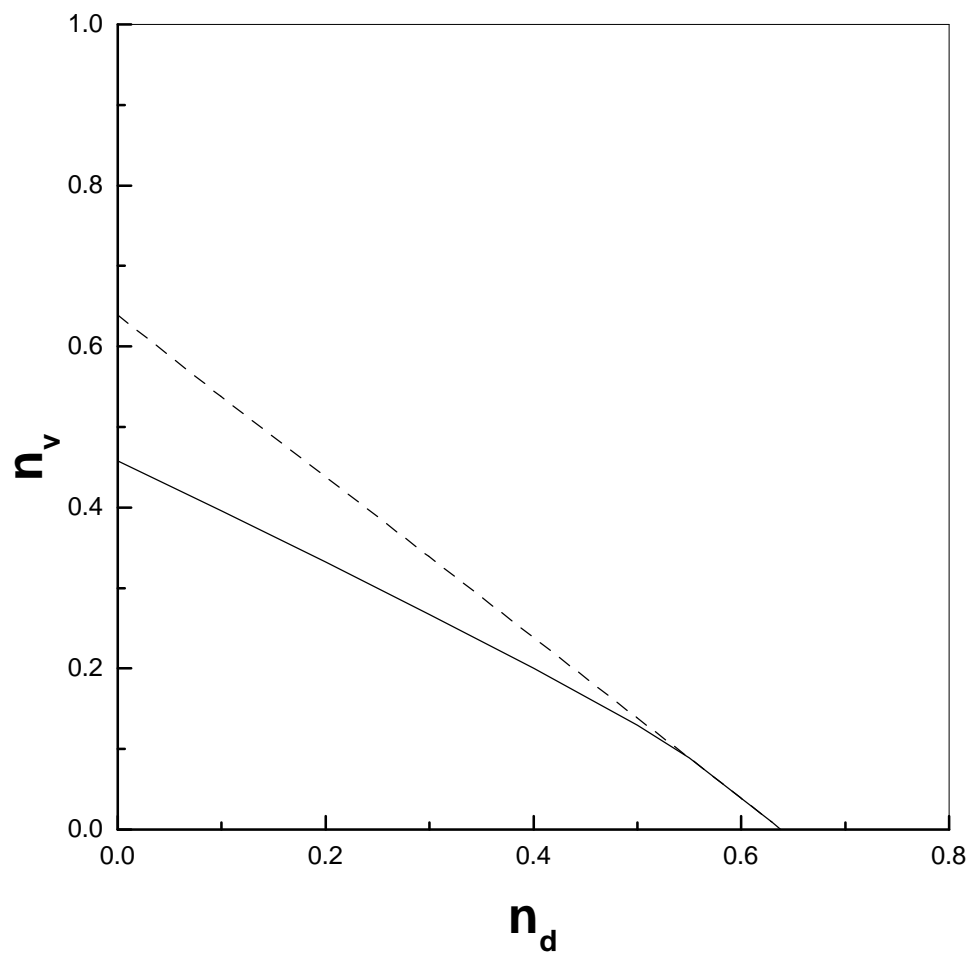


Fig. 5 - Hoenicke + Figueiredo

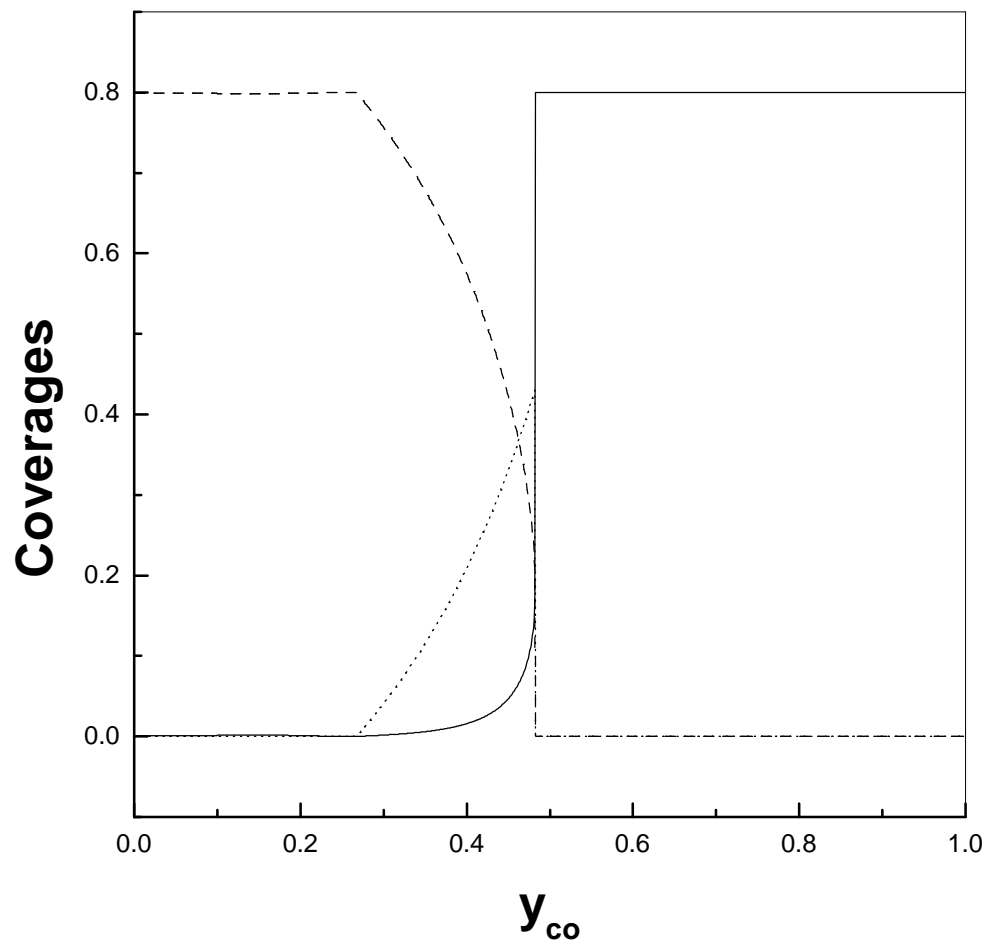


Fig. 6 - Hoenicke + Figueiredo

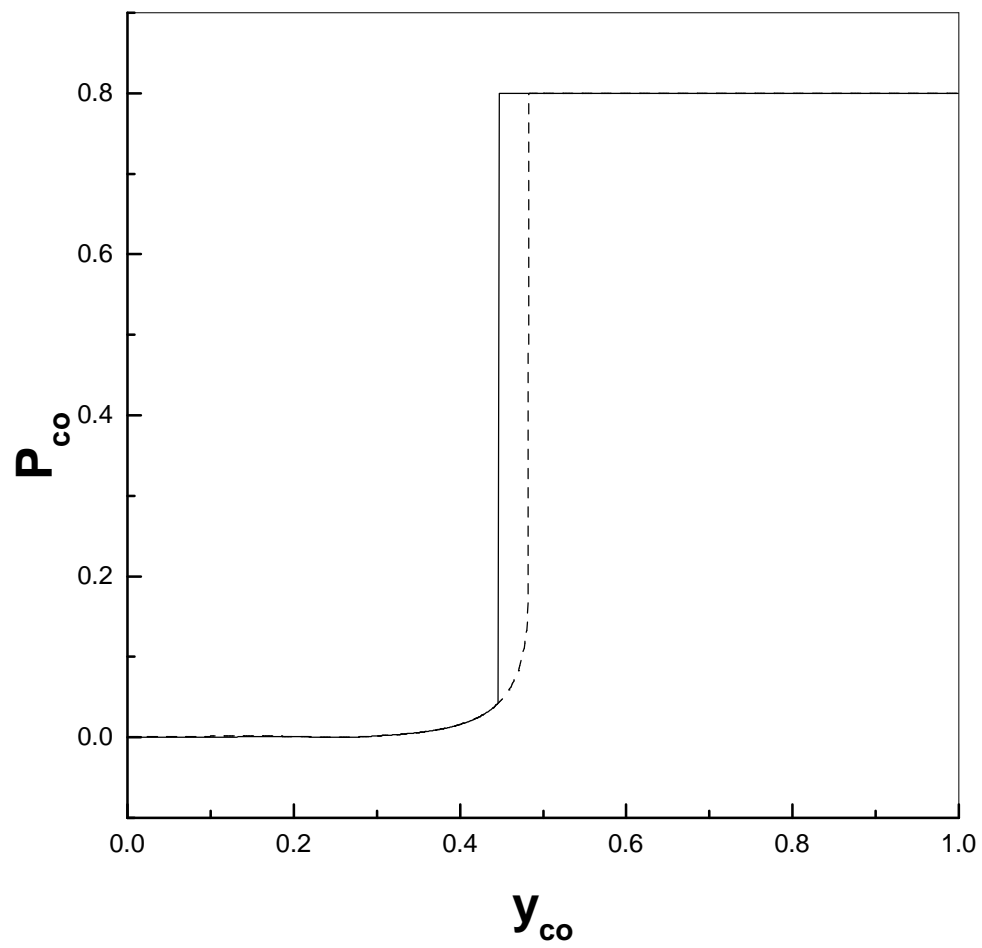


Fig. 7 - Hoenicke + Figueiredo

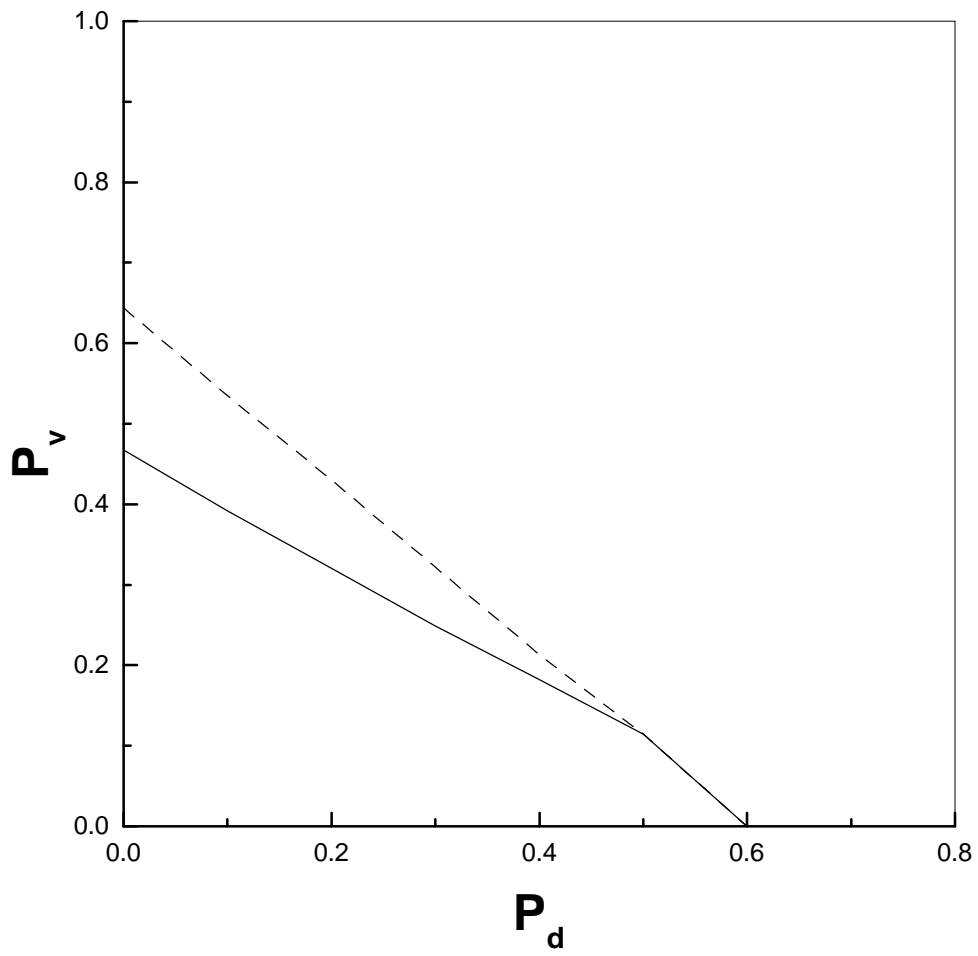


Fig. 8 - Hoenicke + Figueiredo

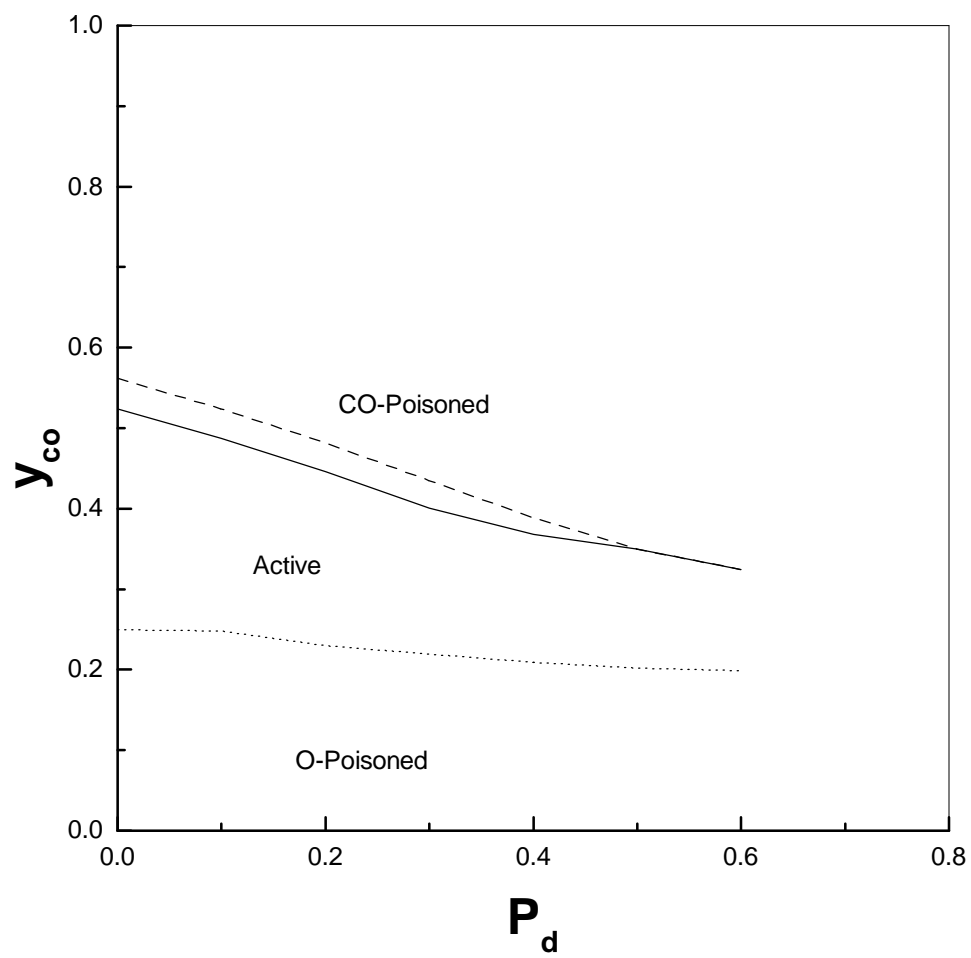


Fig. 9 - Hoenicke + Figueiredo

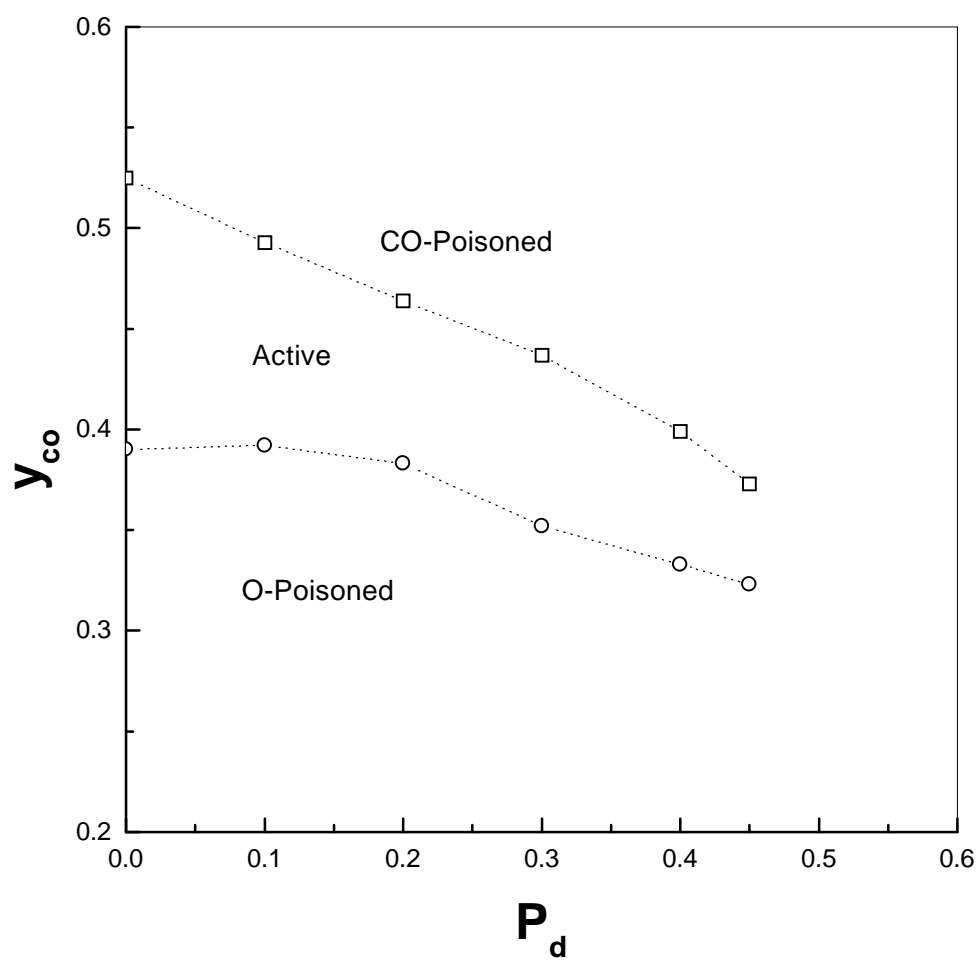


Fig. 10 - Hoenicke + Figueiredo

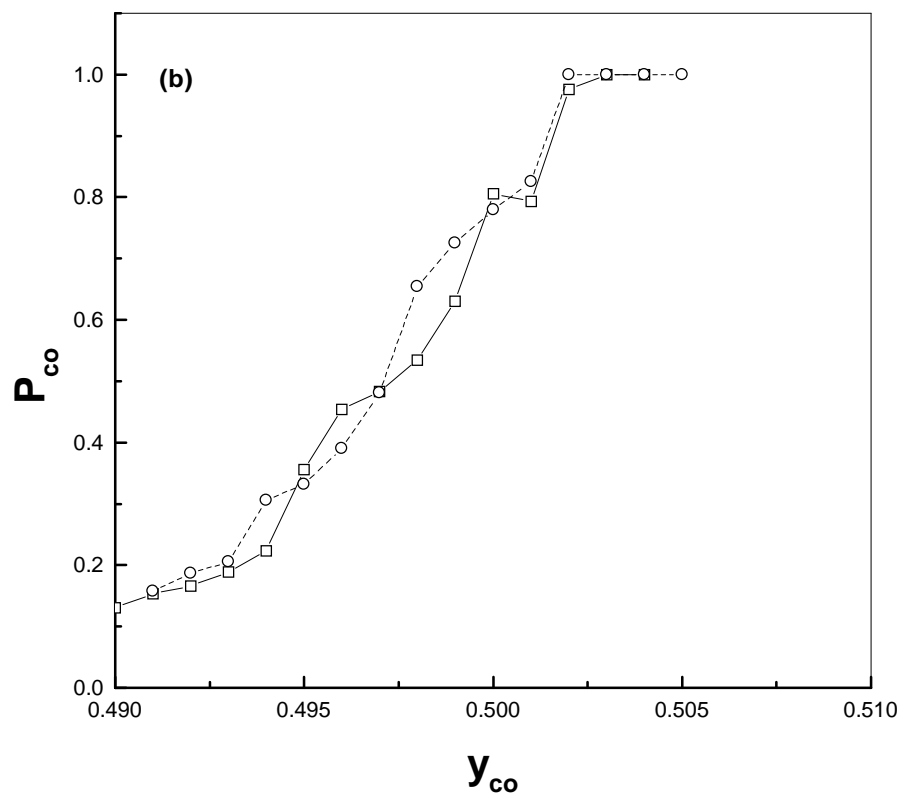
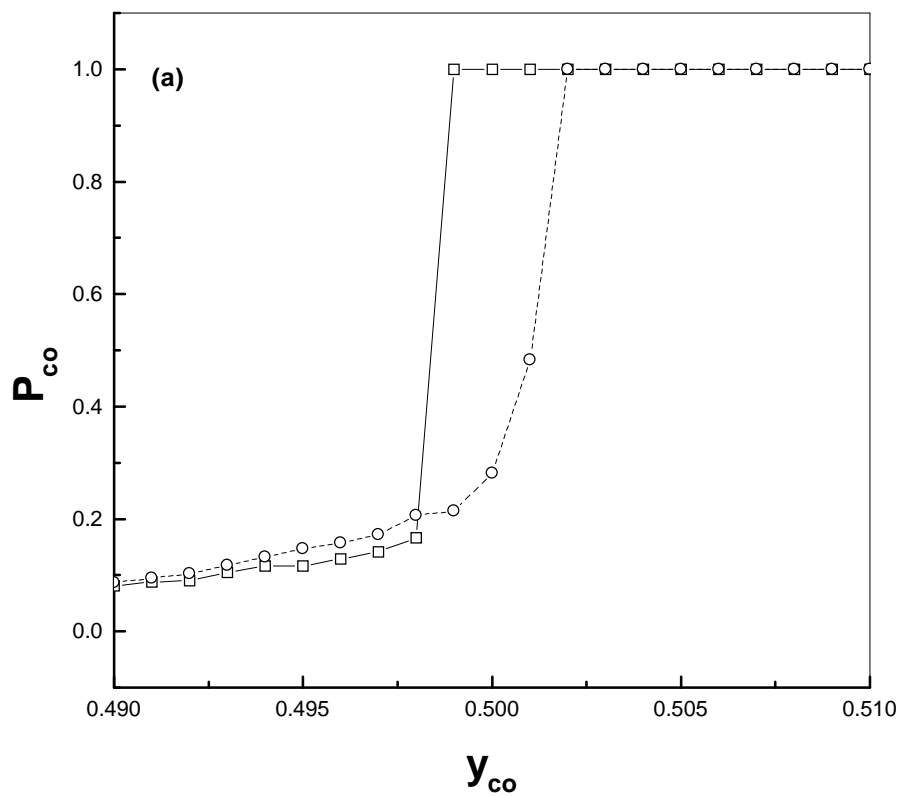


Fig. 11 - Hoenicke + Figueiredo

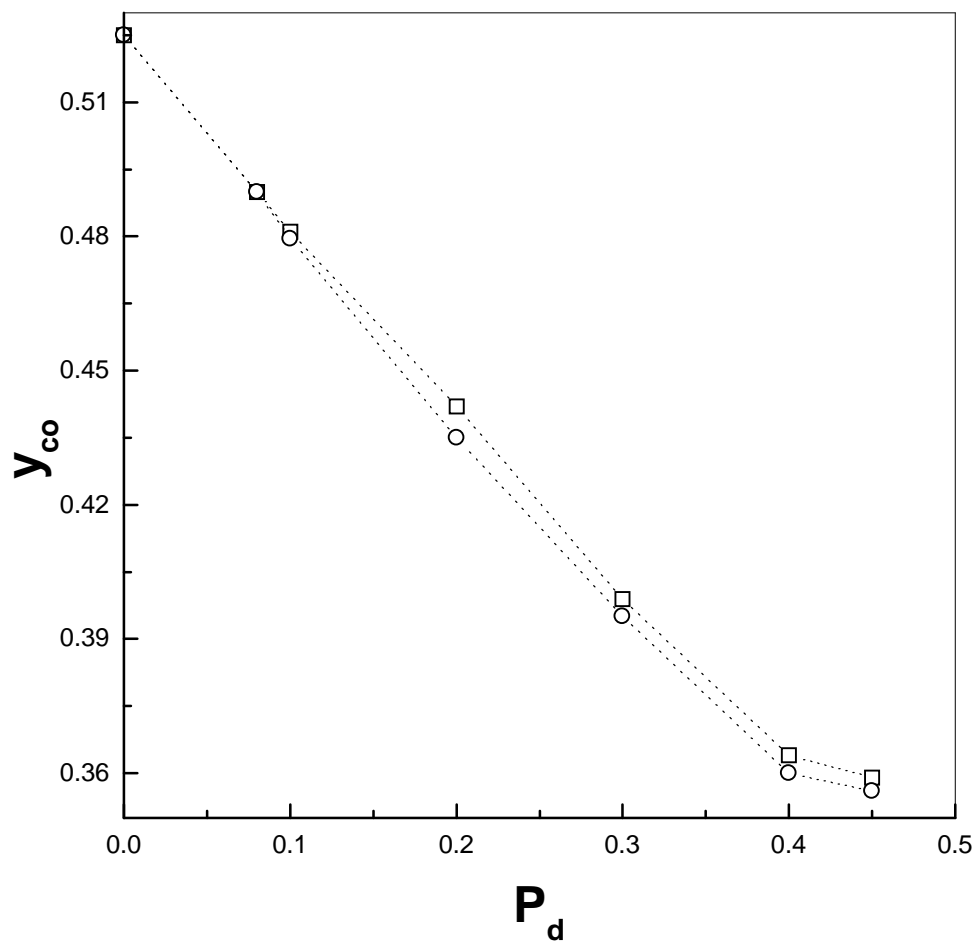


Fig. 12 - Hoenicke + Figueiredo

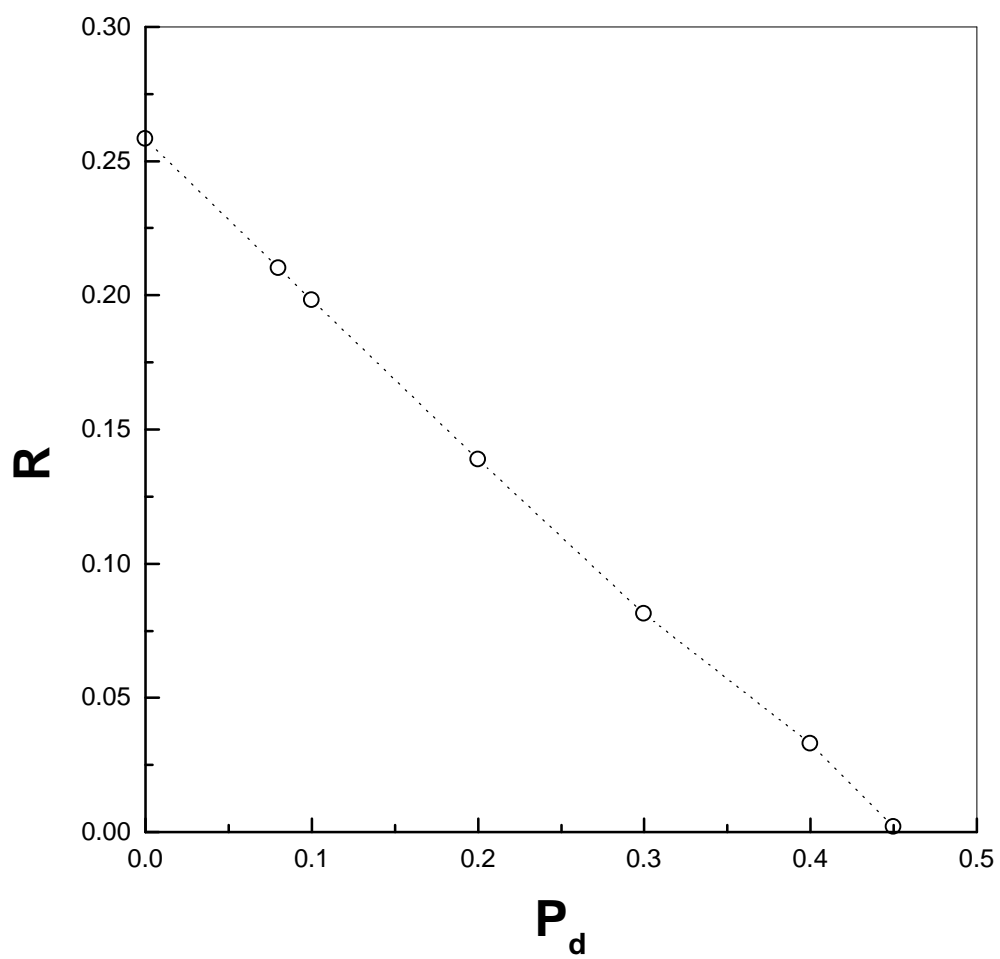


Fig. 13 - Hoenicke + Figueiredo